

Magnetic Properties of Precession Modes Built on High- K Multi-quasiparticle States in ^{178}W

Masayuki MATSUZAKI^{1,*}) and Yoshifumi R. SHIMIZU^{2,**})

¹*Department of Physics, Fukuoka University of Education,
Munakata 811-4192, Japan*

²*Department of Physics, Graduate School of Sciences, Kyushu University,
Fukuoka 812-8581, Japan*

We present an example that shows that the random phase approximation performed on high- K multi-quasiparticle configurations leads to a rotor picture by calculating excitation energies and magnetic properties of ^{178}W . Then we deduce the effective g_R of the high- K rotors and compare it with that of the low- K one.

Rotation is one of typical collective motions in atomic nuclei. Normally axially symmetric nuclei carry large angular momenta in the form of collective rotation about an axis perpendicular to the symmetry axis. In some cases in which single particle orbitals with large angular momenta j_i and their projections to the symmetry axis Ω_i sit at the vicinity of the Fermi surface — realized typically in the $A \sim 180$ region —, the nucleus can have large angular momenta by aligning multiple quasiparticles (QPs) along the symmetry axis. Sometimes the latter scheme forms yrast states, or even if not, isomers are often formed thanks to largeness of $K = \sum_i \Omega_i$.

Detailed information about high- K configurations can be obtained from their magnetic properties — static magnetic moments and/or g -factors inferred from $B(M1)/B(E2)$ branching ratios of in-band transitions in rotational bands excited on top of high- K configurations. The latter data are transformed into $|g_K - g_R|/Q_0$ by way of the rotor model.¹⁾ Then by assuming appropriate g_R and Q_0 , the extracted g_K is compared with the weighted average of single- j g -factors with respect to Ω_i .²⁾

On the other hand, (at least lower members of) rotational bands excited on high- K configurations can be described as multiple excitations of the precession phonons in the language of the random phase approximation (RPA).^{3),4)} Thus, by calculating the wave function of the one phonon state, $B(M1 : I = K + 1 \rightarrow K)$ can be obtained and transformed into the effective (RPA) $(g_K - g_R)$; its sign can be determined by the calculated $E2/M1$ mixing ratio. The magnetic moment $\langle \mu \rangle$ and accordingly the g -factor, $g = \sqrt{\frac{4\pi}{3}} \langle \mu \rangle / (\langle J \rangle \mu_N)$, of high- K configurations can be calculated in the mean field level. Since this g essentially coincides with g_K , we can deduce g_R of the high- K rotor by combining the RPA $(g_K - g_R)$ and g .

The purpose of the paper is twofold: By applying the above method to ^{178}W for which the richest experimental information⁵⁾⁻⁷⁾ is available, we corroborate that the RPA gives a rotor picture via the excitation energies and magnetic properties, and

*) E-mail: matsuzaki@fukuoka-edu.ac.jp

**) E-mail: yrsh2scp@mbox.nc.kyushu-u.ac.jp

deduce g_R of high- K rotors.

We begin with a one-body Hamiltonian,

$$\begin{aligned} h' &= h - \hbar\omega_{\text{rot}}J_x, \\ h &= h_{\text{Nil}} - \Delta_\tau(P_\tau^\dagger + P_\tau) - \lambda_\tau N_\tau, \\ h_{\text{Nil}} &= \frac{\mathbf{p}^2}{2M} + \frac{1}{2}M(\omega_x^2 x^2 + \omega_y^2 y^2 + \omega_z^2 z^2) + v_{ls}\mathbf{l} \cdot \mathbf{s} + v_{ll}(\mathbf{l}^2 - \langle \mathbf{l}^2 \rangle_{N_{\text{osc}}}). \end{aligned} \quad (1)$$

Here $\tau = 1$ and 2 stand for neutron and proton, respectively, and chemical potentials λ_τ are determined so as to give correct average particle numbers $\langle N_\tau \rangle$. The oscillator frequencies are related to the quadrupole deformation parameters ϵ_2 and γ in the usual way. [We adopt the so-called Lund convention.] The orbital angular momentum \mathbf{l} is defined in the singly-stretched coordinates $x'_k = \sqrt{\frac{\omega_k}{\omega_0}}x_k$, with $k = 1 - 3$ denoting $x - z$, and the corresponding momenta. Nuclear states with QP excitations, *i.e.*, alignments along the x axis, are obtained by exchanging the QP energy and wave functions such as

$$(-e'_\mu, \mathbf{V}_\mu, \mathbf{U}_\mu) \rightarrow (e'_{\bar{\mu}}, \mathbf{U}_{\bar{\mu}}, \mathbf{V}_{\bar{\mu}}), \quad (2)$$

where $\bar{\mu}$ denotes the signature partner of μ .

We perform the RPA to the residual pairing plus doubly-stretched quadrupole-quadrupole ($Q'' \cdot Q''$) interaction between QPs. Since we are interested in the precession mode that has a definite signature quantum number, $\alpha = 1$, only two components out of five of the $Q'' \cdot Q''$ interaction are relevant. They are $K = \pm 1$ components. Note that we call the symmetry axis, with respect to which the K quantum number is defined, the x axis throughout this paper. That is, we consider the $\gamma = -120^\circ$ case. These components of the interaction are related to the restoration of the spherical symmetry. Requiring the decoupling of this symmetry mode (the Nambu-Goldstone mode), $J_\pm = J_y \pm iJ_z$, the strength of the interaction is determined. Then, utilizing the identities in Table III of Ref. 8)*), the RPA equation of motion can be cast into⁹⁾ the following form (3), which we use in the actual calculation rather than the original equation in terms of Q'' operators:

$$(\omega^2 - \omega_{\text{rot}}^2) \begin{vmatrix} A(\omega) & C(\omega) \\ B(\omega) & D(\omega) \end{vmatrix} = 0, \quad (3)$$

where

$$\begin{aligned} A(\omega) &= \omega \mathcal{J}_y(\omega) - \omega_{\text{rot}} \mathcal{J}_{yz}(\omega), \\ B(\omega) &= \omega_{\text{rot}} (\mathcal{J}_y(\omega) - \mathcal{J}_x) - \omega \mathcal{J}_{yz}(\omega), \\ C(\omega) &= \omega_{\text{rot}} (\mathcal{J}_z(\omega) - \mathcal{J}_x) - \omega \mathcal{J}_{yz}(\omega), \\ D(\omega) &= \omega \mathcal{J}_z(\omega) - \omega_{\text{rot}} \mathcal{J}_{yz}(\omega), \end{aligned} \quad (4)$$

*) Strictly speaking, the identities have tiny deviations brought about by the singly-stretched (rather than the non-stretched) $\mathbf{l} \cdot \mathbf{s}$ and \mathbf{l}^2 potentials.

with

$$\begin{aligned}
\mathcal{J}_x &= \hbar \langle J_x \rangle / \omega_{\text{rot}}, \\
\mathcal{J}_y(\omega) &= \sum_{\mu < \nu}^{(\alpha=\pm 1/2)} \frac{2E_{\mu\nu} (iJ_y(\mu\nu))^2}{E_{\mu\nu}^2 - (\hbar\omega)^2}, \\
\mathcal{J}_z(\omega) &= \sum_{\mu < \nu}^{(\alpha=\pm 1/2)} \frac{2E_{\mu\nu} (J_z(\mu\nu))^2}{E_{\mu\nu}^2 - (\hbar\omega)^2}, \\
\mathcal{J}_{yz}(\omega) &= \sum_{\mu < \nu}^{(\alpha=\pm 1/2)} \frac{2\hbar\omega iJ_y(\mu\nu)J_z(\mu\nu)}{E_{\mu\nu}^2 - (\hbar\omega)^2}. \tag{5}
\end{aligned}$$

Here we adopt the convention that matrix elements of J_y and μ_y (below) are pure imaginary. The non-spurious part of Eq. (3), $A(\omega)D(\omega) - B(\omega)C(\omega) = 0$, can be rewritten as

$$\left[\omega \mathcal{J}_+^{(\text{eff})}(\omega) - \omega_{\text{rot}} \left(\mathcal{J}_x - \mathcal{J}_+^{(\text{eff})}(\omega) \right) \right] \left[\omega \mathcal{J}_-^{(\text{eff})}(\omega) + \omega_{\text{rot}} \left(\mathcal{J}_x - \mathcal{J}_-^{(\text{eff})}(\omega) \right) \right] = 0, \tag{6}$$

where the suffixes + and - refer to the $\Delta K = +1$ and -1 modes, respectively, and

$$\begin{aligned}
\mathcal{J}_{\pm}^{(\text{eff})}(\omega) &= \mathcal{J}_{\perp}(\omega) \mp \mathcal{J}_{yz}(\omega), \\
\mathcal{J}_{\perp}(\omega) &= \mathcal{J}_y(\omega) = \mathcal{J}_z(\omega). \tag{7}
\end{aligned}$$

For $\Delta K = +1$ excitations, corresponding to the precession modes, the excitation energy in the laboratory frame is given by

$$\hbar\omega + \hbar\omega_{\text{rot}} = \hbar\omega_{\text{rot}} \frac{\mathcal{J}_x}{\mathcal{J}_+^{(\text{eff})}(\omega)} = \hbar^2 \frac{\langle J_x \rangle}{\mathcal{J}_+^{(\text{eff})}(\omega)}, \tag{8}$$

which is independent of ω_{rot} . Since the excitation energy of the first rotational state on the high- K configuration in the rotor model is given by

$$E_{I=K+1} - E_{I=K} = \frac{\hbar^2}{\mathcal{J}} (K+1) \tag{9}$$

derived from

$$E_I = \frac{\hbar^2}{2\mathcal{J}} (I(I+1) - K^2), \tag{10}$$

Eq. (8) [$\langle J_x \rangle = K$ in the cases of $\gamma = -120^\circ$ or 60°] and Eq. (9) correspond to each other well for $K \gg 1$. In other words, $\mathcal{J}_+^{(\text{eff})}(\omega)$ in our RPA formalism and \mathcal{J} in the axially symmetric rotor model correspond to each other.

Marshalek gave an expression for multipole transition rates, which is valid for $I \gg 1$, in terms of the RPA wave function.¹⁰⁾ In the $M1$ case this reads

$$\begin{aligned}
B(M1 : I \rightarrow I-1) &= \frac{1}{2} \langle [i\mu_y + \mu_z, X_n^\dagger] \rangle^2, \\
\mu_{y(z)} &= \sqrt{\frac{3}{4\pi}} \mu_N \left(g_l l_{y(z)} + g_s^{(\text{eff})} s_{y(z)} \right), \tag{11}
\end{aligned}$$

for the n -th phonon state. Hereafter we concentrate on the precession phonon. By equating this with the expression in the rotor model,¹⁾

$$B(M1 : I = K + 1 \rightarrow K) = \frac{3}{4\pi} \mu_N^2 (g_K - g_R)^2 K^2 \langle IK10 | I - 1K \rangle^2, \quad (12)$$

we obtain the RPA $|g_K - g_R|$. Its sign is determined by that of the calculated $E2/M1$ mixing ratio.

Calculation is performed for all the high- K (4, 6, 8 and 10QP) configurations that exhibit rotational bands; $K^\pi = 13^-, 14^+, 15^+, 18^-, 21^-, 22^-, 25^+, 28^-, 29^+, 30^+$ and 34^+ . The $K^\pi = 13^-, 14^+$ and 15^+ are $2\nu 2\pi$, 18^- is $2\nu 4\pi$, 21^- and 22^- are $4\nu 2\pi$, $25^+, 28^-$ and 30^+ are $4\nu 4\pi$, and 29^+ and 34^+ are $6\nu 4\pi$ configurations.^{6),7)} The model space is $N_{\text{osc}} = 3 - 7$ for neutrons and $2 - 6$ for protons. The strengths of the $\mathbf{I} \cdot \mathbf{s}$ and \mathbf{I}^2 potentials are taken from Ref. 11). The pairing gaps are assumed to be 0.5 MeV for 2QP and 0.01 MeV for 4 and 6QP configurations both for neutrons and protons. The quadrupole deformation is chosen to be $\epsilon_2 = 0.235$ that reproduces in a rough average the value $Q_0 = 7.0$ eb that was assumed in the experimental analyses.^{6),7)} As for the spin g -factor, $g_s^{(\text{eff})} = 0.7g_s^{(\text{free})}$ is adopted as usual. These mean that the choice of parameters in this work is semi-quantitative; we checked the robustness of the results with respect to their variations. In the cases symmetric about the x axis considered here the results do not depend on ω_{rot} , while actual calculations are performed at $\hbar\omega_{\text{rot}} = 0.001$ MeV.

Figure 1 presents the calculated and observed relative excitation energies of the first rotational band members, $E_{I=K+1} - E_{I=K}$. Our RPA calculation reproduces their gross features well but with a close look one finds deviations at $K^\pi = 18^-, 25^+, 28^-$, and 29^+ that include the $\pi h_{9/2}$ orbital. Low calculated energies correspond to large moments of inertia [see Eq. (8)] and their largeness correlates with that of calculated Q_0 . The largeness of Q_0 indicates the shape polarization effect of this high- j orbital to the prolate direction. As for the effect of the $\pi h_{9/2}$ orbital on the moment of inertia, see also Refs. 12), 13).

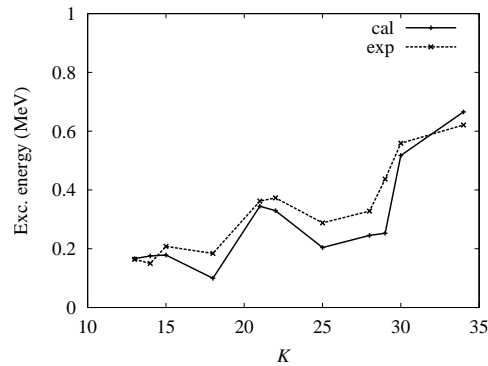


Fig. 1. Calculated and experimental excitation energies of the first rotational band members, $E_{I=K+1} - E_{I=K}$. Data are taken from Refs. 6), 7).

In Fig.2 we compare the RPA ($g_K - g_R$) extracted from the calculated $B(M1; I = K+1 \rightarrow K)$ and the observed one extracted assuming $Q_0 = 7.0$ eb from the branching

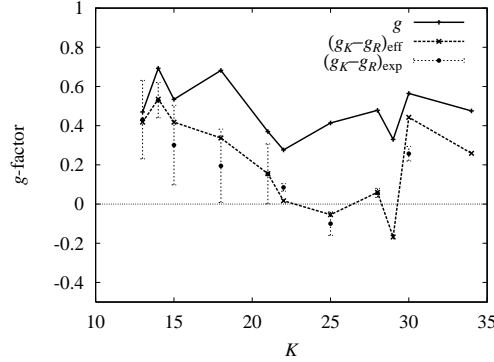


Fig. 2. Calculated intrinsic g of high- K configurations (solid curve) and calculated (dashed curve) and experimental (points with error bars) ($g_K - g_R$). Data are taken from Refs. 6), 7).

ratios of available lowest transitions in respective rotational bands. Their agreement is semi-quantitative. In this figure the calculated intrinsic $g = \sqrt{\frac{4\pi}{3}} \langle \mu_x \rangle / (\langle J_x \rangle \mu_N)$ of high- K configurations are also shown. The two calculated curves roughly correlate. According to the relation¹⁾

$$g_R = g - (g_K - g_R) \frac{K^2}{I(I+1)} \quad (13)$$

with $I = K + 1$, g almost coincides with g_K . Consequently, the difference between the two curves essentially corresponds to the effective g_R for high- K cases. Thus, this correlation suggests a possibility to deduce the effective g_R of the considered high- K configurations by substituting the RPA ($g_K - g_R$) to Eq. (13). Its average value is about 0.29 as seen from Fig.3. This value may be a rough measure of a property of high- K rotors. Moreover, an interesting feature is that there are considerable variations and those for the configurations including the $\pi h_{9/2}$ orbital are larger than others. In order to see it more closely, in Fig.3 we compare them with those calculated from an approximate relation¹⁴⁾

$$g_R = \frac{\mathcal{J}_\pi}{\mathcal{J}_\nu + \mathcal{J}_\pi}, \quad (14)$$

where the neutron and proton part of the effective inertia, the upper sign of Eq. (7), are substituted to \mathcal{J}_ν and \mathcal{J}_π . It is clear that the g_R values deduced from Eqs. (13) and (14) correspond to each other very well, although those from Eq. (14) are much larger for the configurations in which the $\pi h_{9/2}$ orbital is occupied: The contribution to the moment of inertia from the $\pi h_{9/2}$ orbital is large and overestimated in the calculation as mentioned before in the case of excitation energies.

Finally we compare the deduced g_R of high- K rotors above and that of the ground state band. We calculate g of the 2^+ , 4^+ , and 6^+ states, which to the zeroth approximation plays a role of g_R for the nearby $K \neq 0$ configurations, at $\hbar\omega_{\text{rot}} = 0.053$, 0.119 , and 0.176 MeV, respectively, with $\epsilon_2 = 0.235$, $\gamma = 0$, and the odd-even mass differences $\Delta_n = 0.883$ MeV and $\Delta_p = 1.026$ MeV as pairing gaps. The

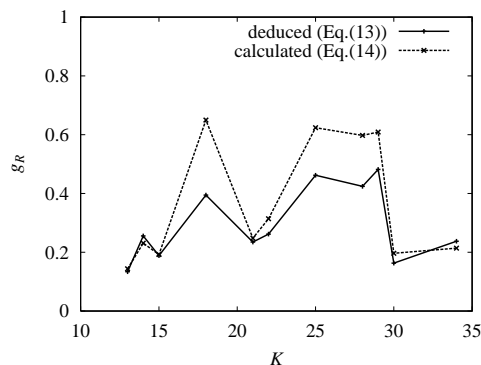


Fig. 3. g_R of high- K rotors deduced using Eq. (13) (solid curve) and calculated using Eq. (14) (dashed curve).

results are $g = 0.218$, 0.216 , and 0.214 , respectively, which almost coincides with the average for the configurations that do not include the $\pi h_{9/2}$ orbital. This indicates that high- K and low- K rotors are similar unless the shape driving $\pi h_{9/2}$ orbital is included.

To summarize, we have numerically verified that the random phase approximation performed on high- K multi-quasiparticle configurations leads to a rotor picture, as previously discussed via $E2$ properties by Andersson *et al.*,³⁾ by calculating excitation energies and $M1$ properties. Next we have deduced the effective g_R of the high- K rotors and compared them with those of the low- K rotor near the ground state. A more detailed investigation is under progress.

-
- 1) A. Bohr and B. R. Mottelson, *Nuclear Structure Vol. II* (Benjamin, New York, 1975).
 - 2) R. A. Bark *et al.*, Nucl. Phys. A **591** (1995), 265.
 - 3) C. G. Andersson, J. Krumlinde, G. Leander and Z. Szymański, Nucl. Phys. A **361** (1981), 147.
 - 4) J. Skalski, Nucl. Phys. A **473** (1987), 40.
 - 5) C. S. Purry *et al.*, Phys. Rev. Lett. **75** (1995), 406.
 - 6) C. S. Purry *et al.*, Nucl. Phys. A **632** (1998), 229.
 - 7) D. M. Cullen *et al.*, Phys. Rev. C **60** (1999), 064301.
 - 8) Y. R. Shimizu and K. Matsuyanagi, Prog. Theor. Phys. **70** (1983), 144.
 - 9) E. R. Marshalek, Nucl. Phys. A **331** (1979), 429.
 - 10) E. R. Marshalek, Nucl. Phys. A **275** (1977), 416.
 - 11) T. Bengtsson and I. Ragnarsson, Nucl. Phys. A **436** (1985), 14.
 - 12) G. D. Dracoulis, F. G. Kondev and P. M. Walker, Phys. Lett. B **419** (1998), 7.
 - 13) S. Frauendorf, K. Neergård, J. A. Sheikh and P. M. Walker, Phys. Rev. C **61** (2000), 064324.
 - 14) R. Bengtsson and S. Åberg, Phys. Lett. B **172** (1986), 277.